Partial System Identification and Sensor Fusion with the Jaiabot Micro Autonomous Underwater Vehicle

Herbert G. Tanner, Chanaka Bandara, and Matthew C. Gyves

***Abstract*— This paper reports on the first approach to dynamical system modeling, identification, control, and environmental quantity estimation with a new, commercially available, micro-AUV named *Jaiabot*. The Jaiabot is a small and relatively inexpensive marine robotic sensor platform that dives vertically to collect measurements of related to water quality, such as salinity and temperature. The paper presents (i) the first dynamical model for Jaiabot's dive motion estimated based on field-data, (ii) a controller redesign given mission specifications associated with vertical environmental quantity profiling, and (iii) a first underwater implementation of a cooperative Kalman filter that fuses measurements from several Jaiabots to yield a confident estimate of temperature or salinity along a path within the convex closure of the vehicle formation.**

I. Introduction

As the effects of climate change intensify, there is increased demand for accurate and timely prediction and forecasting of environmental processes around coastal regions and estuaries. Existing observational infrastructure is not always adequate to provide accurate environmental intelligence at required spatial and temporal resolutions. More often than not, observational capability relies on a sparse collection of static point-measurement stations, which in conjunction with well parameterized computational models have been serving us well for short-to-mid horizon forecasting, but struggle to capture dynamic phenomena that evolve in relatively small spatio-temporal scales. To monitor such phenomena and capture data of sufficient resolution to appropriately parameterize environmental models, we need new observational capabilities that allow for rapid, in-situ, reconfigurable sensor deployments that can offer adjustable measurement resolution, can resolve environmental gradients, and can track dynamic environmental features and processes.

Being able to measure particular water quality variables at different, varying locations of choice at specific times is an important capability, but is currently a labor-intensive and time-consuming task that can be associated with high costs [1], especially when it involves in-situ samples with expensive equipment which needs to be deployed from appropriately instrumented vessels. From this perspective, micro autonomous underwater vehicles (AUVs) which can be deployed from shore, especially in coordinated formation patterns [2], offer unique advantages, facilitating affordable and scalable field measurement for water-quality monitoring.

Tanner and Bandara are with the Department of Mechanical Engineering at the University of Delaware; Email: {btanner,chanaka}@udel.edu. Gyves is with the U.S. Geological Survey; Email: mgyves@usgs.gov

This work is made possible with support from USGS via award #G23AC00149-00.

One such micro-AUV which shows promise for this type of an environmental monitoring application is the Jaiabot (Fig. 1). The Jaiabot is about a meter long, torpedo-shaped AUV that can achieve top speeds of almost 10 knots on the surface of the water. It uses a single propeller for forward thrust and a rudder surface for yaw steering. The AUV shown in Fig. 1 carries a salinity and temperature sensor, a depth sensor, and is rated for a depth of up to 30 m.

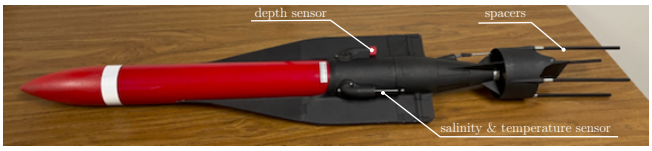

Fig. 1: A Jaiabot micro AUV.

Of particular interest for us is vertical profiling of salinity in environments where sea and freshwater mix. Operationally, salinity can be defined as the concentration of chloride in a liter of water. Salinity undergoes dynamic changes specially in estuary environments. In the Delaware River Basin, a 7-day concentration moving average of 250 mg/l isochlor is set as a regulatory standard because it becomes harmful to freshwater life and is inappropriate for human consumption; this imaginary barrier is known to move by as much as a mile per day in some cases [3]. The intrusion of saltwater from the ocean into the mouth of rivers, like the Delaware river [3], depends on an array of underlying driving processes, including storms, tides, water runoff, and agricultural activity, and can threaten industrial, agricultural, and freshwater intakes as well as fishery and aquaculture activities. Indeed, the salinity gradient determines the boundaries of major biotic and abiotic processes that characterize any estuarine ecosystem [4], [5]. In open water, salinity is critically linked to global climate, the hydrological cycle, and circulation [5].

Most typical salinity measurements are taken as time series at a single deployment point; alternative formats include through manual "grabs" [4], using drifting and towed sensors [6], or via satellite through microwave frequencies (e.g., in open ocean waters) [7]. The recent utilization of robotic sensor platforms for salinity observation has enabled independent validation of satellite-based observations [8], [9]. There is body of work reporting on robotically-assisted water-quality measurement across a column of water. Underwater gliders have occasionally been used for vertical profiling of water-quality characteristics, based on their ability to continuously regulate their depth as they propel

themselves underwater [10]–[13]. In addition to the cost and logistical difficulties of operating and deploying underwater gliders [2], the water-quality data they collect are still sparse if one considers the whole water column (cf. [14]). Vertical profilers (e.g. sondes) deployed using autonomous surface vehicles (ASVs) [15]–[17] may not be faced with this data extrapolation issue, yet compared to a single platform system they represent a more costly and complex solution, which may also be influenced by weather and sea state conditions. There is a subset of work that is going beyond just sampling to employ sensor fusion and distributed field estimation tools that are applicable in a marine environmental observation setting [18]–[21]; indeed, estimation of water quality through distributed sensor fusion and filtering is important to reduce measurement noise and provide more confident estimates of 2D and 3D channel dynamics. However most of this work has been developed for and demonstrated in planar (water surface) settings.

The need for high-resolution depth-profiling measurements, especially in regions such as the Mid-Atlantic, is known and documented [22]. Our ultimate goal is to provide additional tools to respond to this need, that combine sampling with sensor fusion and filtering, using the Jaiabot as a versatile, rapid-deployment sensor platform for vertical profiling of water salinity. In doing that, we are faced with an opportunity and a challenge: on one hand, the particular AUV is suited for quick deployment and is capable of steering itself in strong current environments as those occasionally found in rivers and coastal regions; on the other hand, the vehicle's dynamics are not by default tuned for underwater maneuvering that is conducive to producing the group formations that are ideal for sensor fusion from spatially distributed measurements.

The *contributions* of this paper are identified on the field robotics domain and are outlined as follows:

- The *identification* of the first dynamical model for the Jaiabot in vertical dive;
- The model-based *control redesign* for diving with new *safety and sustainability* specifications in mind;
- The demonstration of environmental multi-sensor *underwater data fusion*, as enabled by the new diving control loop.

The remaining of the paper is organized as follows. Section II frames the technical problem that is addressed in this work. Section III outlines the technical approach followed to provide the solution to the problem stated, and is followed by Section IV which provides experimental evidence in support of the efficacy of the proposed solution. Section V closes the paper summarizing the research outcomes and reflecting on them for future work.

II. Problem Statement

The Jaiabot AUV dives vertically, with its propeller applying negative thrust, oriented in a way that its nose is pointing up toward the surface and its propeller is pointing toward the bottom. The purpose of the spacers shown in Fig. 1 are to protect the propeller and rudder control surfaces from hard contact with the bottom substrate.

Here lies one of the main reasons motivating this work. While any reasonable feedback control loop on the AUV depth can eventually stabilize the AUV at a desired reference depth, data acquisition near the bottom can become problematic if significant *overshoot* is present in the vehicle's transient response. Depending on the nature of the benthic substrate, a high speed overshoot and subsequent contact can cause the vehicle to partially burry itself there if the bottom consists of loose sand or mud; it may result in structural damage to the AUV if the bottom is rocky; or it may also cause environmental damage if the bottom harbors a fragile ecosystem such as a corral reef. In addition to be able to protect the benthic environment as well as the vehicle, it would also be desirable to be able to settle at desired depths in at most 10 seconds, as this feature would facilitate shorter deployments with preservation of vehicle battery and personnel time in the field.

With these considerations in mind, we frame the technical problem as follows:

Problem 1: Design a diving controller for the Jaiabot that exhibits minimal to no overshoot and showcases a settling time of approximately 5 seconds.

In view of Problem 1, it becomes clear that there is another associated problem that has to be addressed in advance: system identification.

Problem 2: Identify the Jaiabot dynamics during its vertical diving phase.

The section that follows presents an experimental approach to addressing Problem 2 first, and then given the solution constructed, proceeds with a model-based design in response to Problem 1.

III. Technical Approach

The vertical diving feature of the Jaiabot offers an opportunity to expediently address Problems 2 and 1. This is because the vertical motion during diving decouples the different degrees of freedom of the AUV and allows one to focus exclusively on the vehicle's surge (forward) dynamics.

A. System Identification

For this surge dynamics, we assume a second order (cf. [23]) parametric model template

$$\ddot{x} + a\dot{x} + bx = u \ , \tag{1}$$

where x denotes depth in meters, u is the control acceleration thrust provided by the AUV's propeller in meters per second squared, and $\theta \triangleq (a, b)$ represent constant model parameters, with θ ranging in $\mathbb{R}^2$ and left to be identified.

The first dataset used comes from a unit step response of the Jaiabot with its depth PID controller set at its default settings of $K_p = 10$, $K_i = 1.6$ and $K_d = 12.8$. One instance of this behavior, on a fresh water dive has produced the time series shown in Fig. 2. Noticeable are the significant overshoot and the relatively long settling times. The 80% overshoot is arguably more concerning than the settling time,

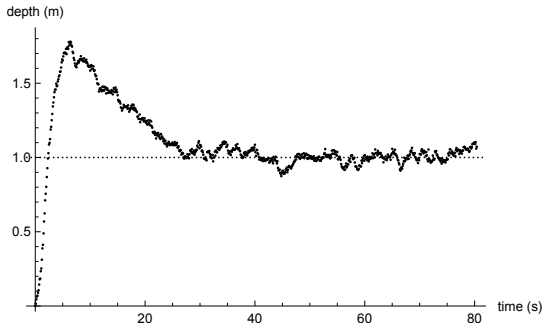

Fig. 2: Depth data from an AUV unit step response with its default PID gains.

and in principle could be attributed to a host of (possibly compounding) factors that include non-unity system steady-state gain and integrator windup. To account for the latter possibility, we designed and tested a PD controller with the following tuning: $K_p = 8.32$, and $K_d = 19.12$. The step response in fresh water with that configuration is shown in Fig. 3, indicating a steady-state gain for the closed loop system that is significantly larger than one.

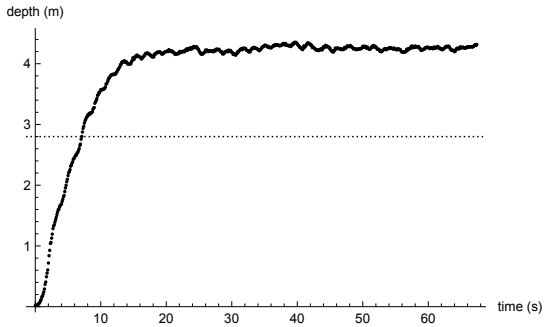

Fig. 3: Depth data from an AUV response at a step input of magnitude 2.8 using a PD controller.

The application of a PD controller leads to a second order closed loop system that enables a more accurate frequency response controller (re)design. For this reason, the data time series of the PD closed loop design featured in Fig. 3 is adopted for an initial system identification. To that end, (1) leads to a frequency response model template for the Jaiabot

$$G_p(s,\theta) = \frac{1}{s^2 + as + b} \ ,$$

and a closed loop parameterized transfer function

$$G_{cl}(s,\theta) = \frac{K_d\, s + K_p}{s^2 + (K_d + a)\, s + (K_p + b)} \ , \qquad (2)$$

with a DC gain of $\frac{K_p}{K_p+b}$. We thus expect a negative value for b suggesting an open-loop unstable transfer function G_p.

At this point, gray-box linear system identification methods [24] applied to (2), utilizing an input-output data time series that subjected the system to a step input of magnitude $|u| = 4.2\ {}^{\mathrm{m}}/_{\mathrm{s}^2}$ yields a parameter estimate of $\theta = (31.11, -2.97)$ with a fit of 70.5% (Fig. 5).

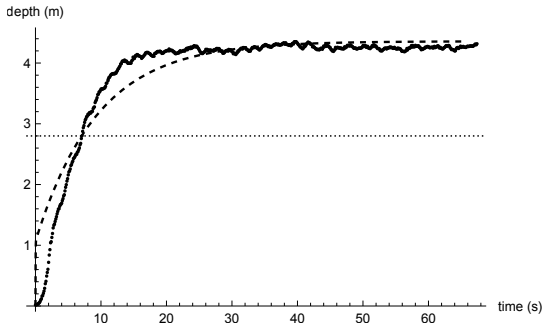

Fig. 4: Comparison of the estimated system model (3) response in closed loop with a PD controller to a 2.8 step input, to the data. Dots: experimental data; dashed line: simulated response of the fitted model.

The estimated model thus takes the form

$$\ddot{x} + 31.11\,\dot{x} - 2.97\,x = u$$
$$\implies G_p(s) = \frac{1}{s^2 + 31.11\,s - 2.97} \ . \qquad (3)$$

Going back to the full PID unit step response of Fig. 2 we can see that the model reasonably captures the high overshoot, albeit not completely; part of the overshoot can actually be due to PID integrator windup which may not be fully captured in simulation.

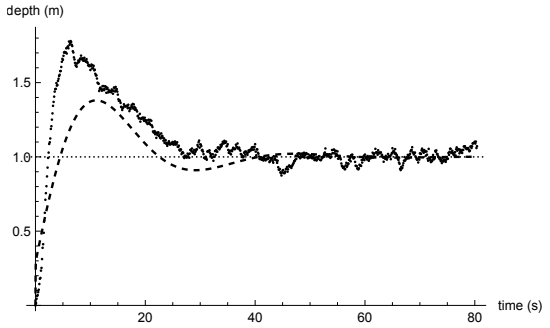

Fig. 5: Comparison of the estimated system model (3) unit step response when in closed loop with a PID controller, to the data. Dots: experimental data; dashed line: simulated response of the fitted model.

B. Controller design

The possibility of integrator windup, and the practical inability (at least at this stage) to implement anti-windup mitigation measures on the Jaiabot AUV, motivates a conservative control design that does not involve integrative action. Among the design specifications for the new control law is the requirement for minimal to no overshoot and short settling times. Specifically, we aim at 0% overshoot (essentially a critically damped system), and a settling time of $t_s < 10$ seconds. Based on this requirements, and for the open loop system (3), a nominal crossover frequency of 1 ${}^{\mathrm{rad}}/_{\mathrm{s}}$ is targeted with a phase margin of 100 degrees. In the absence of integral action, and given the lack of tolerance

to any overshoot, the non-unity DC gain of the closed-loop system will be compensated by a proportional input scaling.

Based on these requirements, a PD controller is designed in the form

$$G_c(s) = K_d\, s + K_p = 13.28\, s + 31.62 \ , \qquad (4)$$

giving a closed-loop DC gain of 1.104. A closed-loop 1.104^{-1} step response is shown in Fig. 6, indicating a settling time of $t_s \approx 5.5$ seconds and no overshoot.

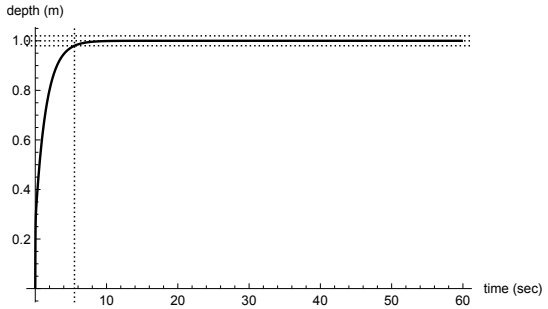

Fig. 6: Simulated unit step response of the identified system model (3) in closed loop with the PD controller (4). Vertical lines mark the unit reference, surrounded by a $\pm 2\%$ margin. The vertical line marks the time when the simulated step response enters the $\pm 2\%$ band around the reference value.

Compared to the original PID step response of Fig. 2, the new control design promises a faster rise and settling time with no overshoot (Fig. 7).

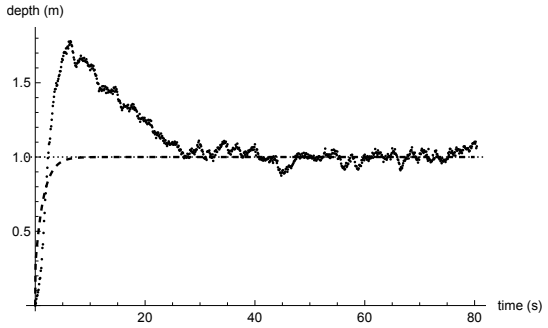

Fig. 7: Simulated step response (dashed line) of the identified system model (3) in closed loop with the PD controller (4), targeted for a unit reference depth, compared with that of the original controller (data points).

C. Cooperative Estimation

The objective here is to perform sensor fusion and cooperative estimation along a vertical plane through the water. Applying a cooperative Kalman filter [19] on data time series collected by AUVs at different depths will allow the estimation of the water-quality parameter of interest at *any* point within the convex hull of the AUV formation. Key to the ability of the cooperative Kalman filter to converge and provide accurate estimates is for the AUV formation to correspond to some particular spatial distribution of vehicles, and for the location of each vehicle to be known with some reasonable accuracy —for instance, we have observed that when the AUVs are positioned significantly off the same vertical plane or are assumed at different depths than the ones they attained, the filtering process may not converge.

The state of the Kalman filter consists of the environmental quantity value and its first spatial derivatives along the (x, y) plane (here: vertical) of observation. If $s(x, y)$ denotes the depth dependent field variable, then the filter state in this case is the vector $\begin{pmatrix} s & \frac{\partial s}{\partial x} & \frac{\partial s}{\partial y} \end{pmatrix}$, and is evaluated at a point in the convex hull of the sensor platform formation denoted $r_c = \begin{pmatrix} x_c & y_c \end{pmatrix}$ —its centroid, by default. The filter's state propagation model, between two subsequent sensor data updates at instants $k-1$ and k is expressed as [19]

$$\begin{pmatrix} s_{[k]} \\ \frac{\partial s}{\partial x}[k] \\ \frac{\partial s}{\partial y}[k] \end{pmatrix} = \begin{bmatrix} 1 & x_{c\,[k]} - x_{c\,[k-1]} & y_{c\,[k]} - y_{c\,[k-1]} \\ 0 & 1 & 0 \\ 0 & 0 & 1 \end{bmatrix} \begin{pmatrix} s_{[k-1]} \\ \frac{\partial s}{\partial x}[k-1] \\ \frac{\partial s}{\partial y}[k-1] \end{pmatrix} + \begin{pmatrix} 0 \\ \mathbb{E}\left\{ (x_{c[k]} - x_{c[k-1]}) \frac{\partial^2 s}{\partial x^2} + (y_{c[k]} - y_{c[k-1]}) \frac{\partial^2 s}{\partial x \partial y} \right\} \\ \mathbb{E}\left\{ (y_{c[k]} - y_{c[k-1]}) \frac{\partial^2 s}{\partial y^2} + (x_{c[k]} - x_{c[k-1]}) \frac{\partial^2 s}{\partial y \partial x} \right\} \end{pmatrix} + \boldsymbol{\epsilon}_{[k-1]} \ , \qquad (5)$$

where $\mathbb{E}\{\cdot\}$ denotes expectation, and $\boldsymbol{\epsilon}$ is assumed to be a Gaussian, independent identically distributed (i.i.d.) zero mean vector representing random modeling errors. The filter's measurement equation, with $p_{i[k]}$ denoting the field measurement of AUV i at time step k, is taken to be

$$\begin{pmatrix} p_{i[k]} \\ \vdots \\ p_{n[k]} \end{pmatrix} = \underbrace{\begin{bmatrix} 1 & x_{i[k]} - x_{i[k-1]} & y_{i[k]} - y_{i[k-1]} \\ \vdots & \vdots & \vdots \\ 1 & x_{n[k]} - x_{n[k-1]} & y_{n[k]} - y_{n[k-1]} \end{bmatrix}}_{C_{[k]}} \begin{pmatrix} s_{[k]} \\ \frac{\partial s}{\partial x}[k] \\ \frac{\partial s}{\partial y}[k] \end{pmatrix} + D_{[k]} \left(\begin{pmatrix} \frac{\partial^2 s}{\partial x^2}[k] \\ \frac{\partial^2 s}{\partial x \partial y}[k] \\ \frac{\partial^2 s}{\partial y \partial x}[k] \\ \frac{\partial^2 s}{\partial y^2}[k] \end{pmatrix} + \boldsymbol{e}_{[k]} \right) + \boldsymbol{w}_{[k]} + \boldsymbol{n}_{[k]} \ , \qquad (6)$$

where $\boldsymbol{e}$ denotes the (random) estimation error on the field value's Hessian, $\boldsymbol{w}$ is a vector of (assumed colored) noise, and $\boldsymbol{n}$ a white, zero-mean Gaussian noise vector with i.i.d. components, and

$$D_{[k]} \triangleq \begin{bmatrix} (x_{1[k]} - x_{c[k]})^2 & (x_{1[k]} - x_{c[k]})(y_{1[k]} - y_{c[k]}) & (x_{1[k]} - x_{c[k]})(y_{1[k]} - y_{c[k]}) & (y_{1[k]} - y_{c[k]})^2 \\ \vdots & \vdots & \vdots & \vdots \\ (x_{n[k]} - x_{c[k]})^2 & (x_{n[k]} - x_{c[k]})(y_{n[k]} - y_{c[k]}) & (x_{n[k]} - x_{c[k]})(y_{n[k]} - y_{c[k]}) & (y_{n[k]} - y_{c[k]})^2 \end{bmatrix} .$$

As evident in (5)–(6), the operation of the filter relies on an estimation of the environmental field's Hessian matrix, which can be done directly for a formation of size $n \geq 4$ [19] using an algorithm, a final step of which involves the solution of

an equation for the determination of $\frac{\partial^2 s}{\partial y^2}$. In that equation, $\frac{\partial^2 s}{\partial y^2}$ is multiplied by $(y_i - y_c)^2$ and when this factor tends to zero because of the instantaneous spatial arrangement of the AUVs, the equation becomes ill-conditioned relative to $\frac{\partial^2 s}{\partial y^2}$. Thus in a minor but consequential departure from the original methodology [19] that suggested using all sensor measurements for the determination of $\frac{\partial^2 s}{\partial y^2}$, here we implement a variation of this Hessian estimation algorithm where we take into account only the sensor at AUV i with $i = \arg\max_{i=1,\ldots,n}(x_i - x_c)^2(y_i - y_c)^2$. With the proposed modification the cooperative Kalman filter exhibited robust operation irrespectively of sensor platform deployment and formation configuration.

IV. Experimental Results

Fig. 8: Four Jaiabots, ready to be deployed on a cooperative estimation mission, on the pier by Lake Allure, PA.

Experiments were conducted in lake Allure, PA, that offers sufficient depths to deploy a vertical formation of AUVs. For these tests, four Jaiabots were deployed in lake Allure (Fig. 8) on a cooperative estimation mission in December 2023.

The dynamics of the sensor itself play a role in the estimation process. Sensor data are to be associated to a particular GPS location and specific depth, and knowledge of sensor dynamics, e.g., of sensor response delays, allow for accurate association of measurement to location. Here, however, without specific information regarding the bandwidth of the particular salinity sensor on the Jaiabot it is preferable to let the AUV settle at a given depth before taking the sensor data into consideration. On the other hand, in the calm waters of lake Allure, PA, it is reasonable to assume that there are no currents to carry the submerged AUVs away from the location where they started their dive.

Being a fresh water lake, however, lake Allure does not allow for a meaningful estimation of salinity measurements. For that reason, we used temperature as a sensor data surrogate. In winter months, bodies of fresh water are expected to exhibit some temperature stratification which we hoped to capture in our experimental data. The setup for the AUV formation used for estimation is shown in Fig. 9 for the four Jaiabots indexed 3, 12, 13, and 14.

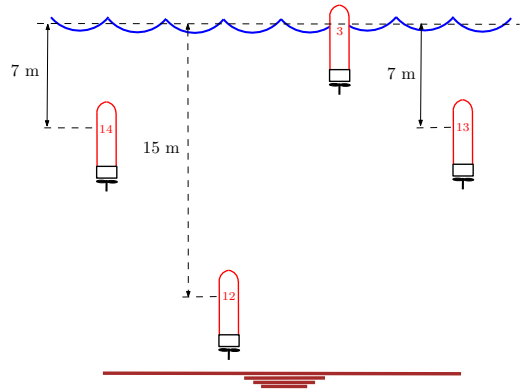

Fig. 9: The target sensor platform formation on cooperative estimation for vertical profiling. The AUVs are equally spaced along the horizontal direction.

As the AUVs settled at their desired depths, time series of temperature measurements were collected. Figure 10 illustrates the process of the Kalman filter convergence on the four color-coded AUV sensor data time series, and an estimate for the temperature at the center of the vehicle formation, starting from a temperature value lower than measurements.

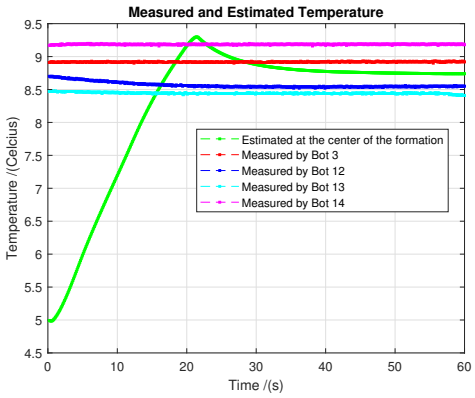

Fig. 10: Four time series of temperature measurements by each AUV at their designated depth, and a cooperative Kalman filter estimate for the temperature at the center of the formation during this time period, when the filter is initiated at a temperature of $T_0 = 5^\circ$ C.

Figure 11 shows a similar process of convergence as that of Fig. 10 but from a different initial condition for the filter, this time higher than the measurement values, demonstrating the ability of the filter to converge in a timely fashion independently of initialization.

V. Conclusion

This paper demonstrated the capability of a coordinated AUV sensor network to perform vertical profiling of spatially distributed scalar environmental fields, providing confident and accurate cooperative estimates of the quantity of interest. A new proof of concept system was developed around the

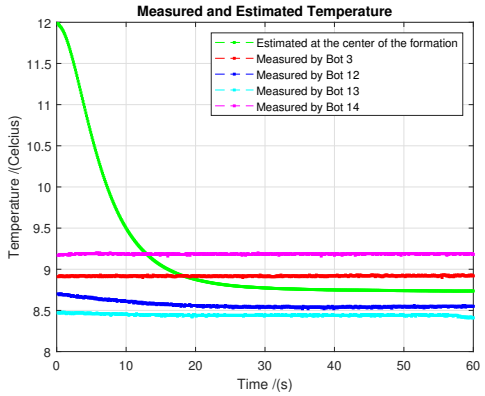

Fig. 11: Four time series of temperature measurements by each AUV at their designated depth, and a cooperative Kalman filter estimate for the temperature at the center of the formation during this time period, when the filter is initiated at a temperature of $T_0 = 12^\circ$ C.

Jaiabot micro-AUV sensor platform for the ultimate purpose of salinity profiling, and was tested in a fresh water environment using water temperature as a surrogate environmental field. Three innovations were introduced in this paper as part of this system development: (i) an experimental data-based system identification of the Jaiabot's surge dynamics; (ii) a design of a new control law for the AUV's diving mode which adheres to platform and environmental safety and sustainability specifications, and (iii) a modification to the cooperative Kalman filtering used for data fusion and field estimation, that circumvents a potential numerical problem which can arise in the process of estimation of the field's Hessian matrix components. An alternative to the proposed solution to the singularity problem in the Hessian element determination for cooperative estimation could be the imposition of a formation control constraint on the AUVs; however, in the particular underwater deployment scenario considered here, where there could be no position telemetry nor underwater communication between the AUVs, the enforcement of such a constraint would have been problematic.

REFERENCES

[1] B. Howe and T. K. Chereskin, "Oceanographic measurements," in *Springer Handbook of Experimental Fluid Mechanics*, C. Tropea, A. L. Yarin, and J. F. Foss, Eds. Springer, 2007, ch. 18, pp. 1179–1217.

[2] H. S. Lim, A. Filisetti, A. Marouchos, K. Khosoussi, and N. Lawrance, "Applied research directions of autonomous marine systems for environmental monitoring," in *OCEANS 2023 – Limerick*, 2023, pp. 1–10.

[3] S. Cook, J. Warner, and K. Russell, "Effects of storms and bathymetry on salinity intrusion in the Delaware Bay estuary," in *Ocean Sciences Meeting*, 2022.

[4] V. Telesh and V. V. Khlebovich, "Principal processes within the estuarine salinity gradient: A review," *Marine Pollution Bulletin*, vol. 61, pp. 149–155, 2010.

[5] C. Woody, E. Shih, J. Miller, T. Royer, L. P. Atkinson, and R. Moody, "Measurements of salinity in the coastal ocean: A review of requirements and technologies," *Marine Technology Society Journal*, vol. 34, no. 2, pp. 26–33, 2000.

[6] V. Hormann, L. Centurioni, A. Mahadevan, S. Essink, E. D'Asaro, and B. P. Kumar, "Variability of near-surface circulation and sea surface salinity observed from Lagrangian drifters in the northern Bay of Bengal during the waning 2015 southwest monsoon," *Oceanography*, vol. 29, no. 2, pp. 124–133, 2016.

[7] J. Boutin, N. Reul, J. Koehler, A. Martin, R. Catany, S. Guimbard, F. Rouffi, J. L. Vergely, M. Arias, M. Chakroun, G. Corato, V. Estella-Perez, A. Hasson, S. Josey, D. Khvorostyanov, N. Kolodziejczyk, J. Mignot, L. Olivier, G. Reverdin, D. Stammer, A. Supply, C. Thouvenin-Masson, A. Turiel, J. Vialard, P. Cipollini, C. Donlon, R. Sabia, , and S. Mecklenburg, "Satellite-based sea surface salinity designed for ocean and climate studies," *JGR Oceans*, vol. 126, no. 11, p. e2021JC017676, 2021.

[8] J. Vazquez-Cuervo, C. Gentemann, W. Tang, D. Carroll, H. Zhang, D. Menemenlis, J. Gomez-Valdes, M. Bouali, and M. Steele, "Using Saildrones to validate arctic sea-surface salinity from the SMAP satellite and from ocean models," *Remote Sensing*, vol. 13, no. 831, 2021.

[9] J. Vazquez-Cuervo, J. Gomez-Valdes, and M. Bouali, "Comparison of satellite-derived sea surface temperature and sea surface salinity gradients using the Saildrone California/Baja and North Atlantic Gulf Stream deployments," *Remote Sensing*, vol. 12, no. 1839, 2020.

[10] R. N. Smith, E. C. Das, H. Heidarsson, A. M. Pereira, F. Arrichiello, I. Cetnic, L. Darjany, M.-E. Garneau, M. D. Howard, C. Oberg, M. Ragan, E. Seubert, E. C. Smith, B. A. Stauffer, A. Schnetzer, G. Toro-Farmer, D. A. Caron, B. H. Jones, and G. S. Sukhatme, "USC CINAPS builds bridges," *IEEE Robotics and Automation Magazine*, vol. 17, no. 1, pp. 20–30, 2010.

[11] R. N. Smith, M. Schwager, S. L. Smith, B. H. Jones, D. Rus, and G. S. Sukhatme, "Persistent ocean monitoring with underwater gliders: Adapting sampling resolution," *Journal of Field Robotics*, vol. 28, no. 5, pp. 714–741, 2011.

[12] K.-C. Ma, Z. Ma, L. Liu, and G. S. Sukhatme, "Multi-robot informative and adaptive planning for persistent environmental monitoring," in *Distributed Autonomous Robotic Systems: The 13th International Symposium*, R. Groß, A. Kolling, S. Berman, E. Frazzoli, A. Martinoli, F. Matsuno, and M. Gauci, Eds. Springer, 2018, pp. 285–298.

[13] N. E. Leonard, D. A. Paley, R. E. Davis, D. M. Fratantoni, F. Lekien, and F. Zhang, "Coordinated control of an underwater glider fleet in an adaptive ocean sampling field experiment in Monterey Bay," *Journal of Field Robotics*, vol. 27, no. 6, pp. 718–740, 2010.

[14] J. A. Breier, M. V. Jakuba, M. A. Saito, G. J. Dick, S. L. Grim, E. W. Chan, M. R. McIlvin, D. M. Moran, B. A. Alanis, , A. E. Allen, C. L. Dupont, and R. Johnson, "Revealing ocean-scale biochemical structure with a deep-diving vertical profiling autonomous vehicle," *Science Robotics*, vol. 5, no. eabc7104, pp. 1–13, 2020.

[15] Y. Huang, Y. Yao, J. Hansen, J. Mallette, S. Manjanna, G. Dudek, , and D. Meger, "An autonomous probing system for collecting measurements at depth from small surface vehicles," in *OCEANS 2021 – San Diego - Porto*, San Diego – Porto, 2021, pp. 1–6.

[16] H. C. Z. G. S. W. H. Cheng and C. Zhan, "Intelligent wide-area water quality monitoring and analysis system exploiting unmanned surface vehicles and ensemble learning," *Water*, vol. 12, no. 681, 2020.

[17] G. Ferri, A. Manzi, F. Fornai, F. Ciuchi, and C. Laschi, "The HydroNet ASV, a small-sized autonomous catamaran for real-time monitoring of water quality: From design to missions at sea," *IEEE Journal of Oceanic Engineering*, vol. 40, no. 3, pp. 710–726, 2014.

[18] M. Santos, U. Madhushani, A. Benevento, and N. E. Leonard, "Multi-robot learning and coverage of unknown spatial fields," in *Proceedings of the International Symposium on Multi-Robot and Multi-Agent Systems*, 2021, pp. 137–145.

[19] F. Zhang and N. E. Leonard, "Cooperative filters and control for cooperative exploration," *IEEE Transactions on Automatic Control*, vol. 55, no. 3, pp. 650–663, 2010.

[20] T. Salam and M. A. Hsieh, "Heterogeneous robot teams for modeling and prediction of multiscale environmental processes," *Autonomous Robots*, vol. 47, pp. 353–376, 2023.

[21] C. K. Peterson and D. A. Paley, "Distributed estimation for motion coordination in an unknown spatially varying flowfield," *Journal of Guidance, Control, and Dynamics*, vol. 36, no. 3, pp. 896–898, 2013.

[22] K. A. Goldsmith, S. Lau, M. E. Poach, G. P. Sakowicz, T. M. Trice, C. R. Ono, J. Nye, E. H. Shadwick, K. A. StLaurent, and G. K. Saba, "Scientific considerations for acidification monitoring in the U.S. Mid-Atlantic region," *Estuarine, Coastal and Shelf Science*, vol. 225, no. 106189, 2019.

[23] T. I. Fossen, *Handbook of marine craft hydrodynamics and motion control*. John Wiley & Sons, 2011.

[24] L. Ljung, *System Identification: Theory for the User*, 2nd ed. Prentice Hall PTR, 1999.